Simulations of solvation dynamics in simple polar solvents

Eyal Neria and Abraham Nitzan
School of Chemistry, the Sackler Faculty of Science, Tel Aviv University, Tel Aviv, 69978, Israel

(Received 2 October 1991; accepted 10 December 1991)

This paper describes the results of computer simulations of charge solvation dynamics in a Stockmayer solvent (Lennard-Jones spheres with point dipoles at their centers). The solvent molecules are characterized by mass and moment of inertia which can be varied independently, thus providing the possibility to study the separate effects of the rotational and translational solvent motions on the solvation process. We focus on the role played by these degrees of freedom, and on the contributions of different solvation shells around the solute to the solvation process in order to check the validity of recently proposed theories of solvation dynamics. We find that even in this structureless solvent, as in the more structured solvents studied earlier, inertial effects dominate the solvation process, and dielectric solvation theories which do not take into account these effects cannot describe the observed dynamics. The dynamic mean spherical approximation and generalized diffusion theories cannot account for the observed dynamics even when solvent translations are frozen.

I. INTRODUCTION

Considerable attention has been focused lately on questions related to the dynamics of charge (and charge distributions) solvation in polar solvents.[1-3] Progress in fast-time experimental techniques has lead to a vast amount of new data on solvation processes in protic and nonprotic solvents, and recent theoretical investigations based on analytical approximations,[4-20] as well as numerical simulations,[21-28] have lead to new insight concerning the nature of the solvation process. The following issues (some of which are interrelated) have been repeatedly discussed.

To what extent can the solvation process be described by continuum dielectric theory and what are the signatures of the solute and solvent structure in the deviation of the observed dynamics from that predicted by continuum dielectric theory?

To what extent can the solvation dynamics be accounted for by the information contained in the long-wavelength dielectric function, $\epsilon(\omega) \equiv \epsilon(k=0,\omega)$, mainly by its Debye form,

$$\epsilon(\omega) = \epsilon_\infty + \frac{\epsilon_0 - \epsilon_\infty}{1 + i\omega\tau_D}, \tag{1}$$

which is characterized by the relaxation times τ_D and $\tau_L = (\epsilon_\infty/\epsilon_0)\tau_D$ [$\epsilon_0 = \epsilon(0)$, $\epsilon_\infty = \epsilon(\infty)$].

How well can the solvation process be described by linear response theory? How does dielectric saturation affect the solvation process?

How does solvent "shell structure" about the solute molecule manifest itself in the solvation process? What is the role of cooperativity in the solvent response? How do different *ranges* of solute-solvent interaction affect the solvation dynamics, and can they be accounted for by the calculated wavelength dependent dielectric response?

What are the relative roles played by different degrees of freedom of the solvent motion, in particular, rotation and translation, in the solvation process?

How do *inertial* (as opposed to *diffusive*) solvent motions manifest themselves in the solvation process?

Theoretical work of the past few years has attempted to answer these questions. The main approaches taken can be roughly divided into four categories: (i) the dynamical mean spherical approximation (MSA);[6-9] (ii) generalized diffusion equations (GDE) based on the Vlasov–Smoluchowski equation generalized to take into account both solvent translation and rotation and supplemented by information on the equilibrium solvent structure;[10-13] (iii) a generalized Langevin equation (GLE) framework for calculating the time-dependent density correlation functions of the solvent, again supplemented by input (in the form of the static direct correlation function) about the pure solvent structure;[15] (iv) expressing the solvation energy in terms of $\epsilon(k,\omega)$ and using *ad hoc* assumptions and conjectures about the functional form of the latter.[16] These are essentially linear-response theories, and give, within their imposed limits, similar answers to the aforementioned questions. These theories predict a nonexponential decay of the solvation energy in contrast to the dielectric continuum model (DCM) which, for the Debye solvent [Eq. (1)], predicts an exponential relaxation with characteristic time τ_L. Neglecting translational motion of the solvent, the relaxation times obtained are between τ_L and τ_D and the relaxation is faster and closer to the DCM prediction when solute/solvent size ratio increases. Incorporation of solvent translational motion can yield relaxation times even shorter then τ_L.

Of particular interest is the relation of the different relaxation times to the interaction range and to the solvent shell structure about the solute. Following an early remark made by Onsager[29] that the shorter time scales are associated mostly with solvent layers further away from the solute, and that the longer $\sim\tau_D$ times are associated with the individual response of solvent molecules nearest to the solute, attempts were made to substantiate this assertion by a rigorous calculation. Indeed, for purely rotational models, the

 0021-9606/92/075433-08$06.00

Onsager conjecture has been corroborated by the aforementioned theories. However, Chandra and Bagchi have shown,[12,13] within a GDE framework, that when translational motion is important [$D_T/(2D_R\sigma^2) \geqslant 0.5$, where D_T, D_R, and σ are, respectively, the translational and rotational diffusion coefficients and the molecular diameter of the solvent], then the relaxation is affected by the different solvent shells in a manner opposite to that suggested by Onsager, namely, the fastest dynamics is associated with shells closest to the solute molecule.

Available experimental data can be generally rationalized along these theoretical predictions. Energy shifts associated with solvation relax nonexponentially, with the average relaxation time usually close to that predicted by the DCM (τ_L for a Debye solvent). In several cases[30] the initial relaxation is observed to be faster, in contrast to the predictions of the theories which take into account only orientational relaxation and determine τ_L to be the upper bound on the relaxation times (see, however, Refs. 12 and 13). It should also be kept in mind that the most sophisticated experiments are currently limited to time scales longer then 100–200 fs, so faster relaxation components would not be seen. Obviously, issues concerning the correlation of time and length scales are not easily observable. Neither the Onsager "inverse snowball" behavior, nor the role played by different solvation shells or the relative importance of solvent rotational and translational motions, has thus far been directly verified. These issues have been discussed in the light of recent numerical simulation work.[2,21-28]

Quite a few simulation studies of solvation dynamics and related phenomena have been published recently.[2,21-28] Most of these studies[21-26] were made on computer models of aqueous systems. Two remarkable outcomes of the latter group of simulations are, first, the close agreement between results obtained by different groups simulating different (rigid and nonrigid) water models, and, secondly, the strong disagreement between these simulation results and the predictions of most analytical theories. In contrast to these theories, these simulations show that the relaxation proceeds on at least two time scales, the fastest one is of the order of 25 fs and accounts for 70%–80% of the solvation energy while the other is an order of magnitude slower. Furthermore, these simulations indicate that the fast relaxation is associated with inertial librations of the H atoms, not accounted for in current theories. Naturally, the fact that water is unique in the degree of structure imposed by its H-bond network has been suggested as a cause for this behavior. Recently Maroncelli[2] has performed simulations of solvation dynamics in a model acetonitrile, while Carter and Hynes[27] have performed similar simulations in a diatomic model roughly representing CH_3Cl. Surprisingly, the results of these simulations are qualitatively similar to the water simulations. In particular, Maroncelli[2] considered the dynamics of charge solvation described by either the equilibrium response function

$$C(t) = \frac{\langle \delta V(t) \delta V(0) \rangle}{\langle \delta V^2 \rangle}, \tag{2}$$

where δV is the fluctuation in the electrical potential at the solute position, or the nonequilibrium response function

$$S(t) = \frac{\Delta E_{\text{solv}}(t) - \Delta E_{\text{solv}}(\infty)}{\Delta E_{\text{solv}}(0) - \Delta E_{\text{solv}}(\infty)}, \tag{3}$$

where $\Delta E_{\text{solv}}(t)$ is the solvent–solute interaction energy observed after a step function change in the solute charge, and found that both are characterized by a fast ($\sim$0.05–0.1 ps at room temperature) Gaussian initial relaxation which accounts for $\sim$80% of the relaxation followed by a much slower relaxation (0.5–1 ps) which accounts for the remaining solvation. These time scales should be compared to the dielectric relaxation times for this computer solvent, $\tau_D = 4.1$ ps and $\tau_L = 0.12$ ps. The observed response is thus closer to the DCM prediction then to the MSA result (e.g., $\langle \tau_{\text{MSA}} \rangle = 0.44$ ps for this solvent while the observed $\langle \tau \rangle$ is 0.17 ps); however, it differs from the DCM/Debye model (and from the prediction of the GDE, including translation) in its bimodal character. In addition, the results of Maroncelli exhibit oscillations with a period of $\sim$0.2 ps, resulting from inertial dynamics of solvent molecules close to the solute. Thus, the fast solvation response is dominated by solvation shells closer to the solute and the dynamics proceeds from the inner region to the outside, namely in a "counter Onsager" manner. For the model considered by Maroncelli, roughly twice as much energy flows through the rotational energy channel than through the translational one.

Many of the aforementioned features have also been observed in the study of Carter and Hynes,[27] and appear to be general, at least for small molecule solvents. In particular, the qualitative similarity to simulation of solvation in water is striking. In the latter simulations the fast initial response, which also accounts for most of the solvation, is characterized by a relaxation time of $\sim$20–30 fs, about half of τ_L in the ST2 model used by Maroncelli and Fleming,[22] and about $0.15\tau_L$ in the SPC simulations of Bader and Chandler.[26] Interestingly, the fast relaxation component appears very similar in these two models even though their dielectric relaxation properties are so different. This observation supports the conjecture that the fast relaxation component is associated with inertial (as opposed to diffusional) motions not accounted for in the Debye model of dielectric relaxation (and by simple extensions of it), and suggests that the similarity between the numerical values of τ_L and the fast relaxation component seen in the acetonitrile simulations[2] may be accidental. The strongest evidence for this and for the importance of inertial motions in the fast relaxation component is provided by Maroncelli's comparison[2] between the solvation dynamics in his acetonitrile simulations described earlier, and between his rigid cage simulations (where all but one solvent molecules are frozen) for the same model. A recent theoretical calculation by Chandra and Bagchi[20] also indicates that inertial effects can enhance the early stages of the solvation dynamics (see also Ref. 5). On the experimental side, clear evidence for the importance of inertial motion in the solvation dynamics in acetonitrile has been provided very recently by Rosenthal *et al.*[31]

The apparent generality of the observations described earlier is a somewhat surprising development following ini-

tial expectations that this type of behavior was unique to water and possibly other highly structured H-bonded solvents. The general conceptual picture of the solvation process inferred from the simulations is substantially different from that inferred from the analytical theories mentioned earlier. In particular, with regard to the relative roles taken in the solvation process by diffusional and inertial motions, by translational and rotational motions, and by the different solvation shells. In this context it is of interest to scale down the solvent model and to examine these issues in computer solvents more similar to those assumed by the analytical theories. In this paper we study solvation dynamics in a Stockmayer solvent: A fluid made of spherical particles interacting with each other and with the solute with Lennard-Jones interactions and with dipolar interactions associated with point dipoles located at the sphere centers.[32] The solute is a spherical atom which (for the nonequilibrium simulation) becomes a singly charged ion at $t=0$. The original choice of molecular parameters approximate those of the CH_3Cl molecule, however, the mass and moment of inertia of the solvent molecule have been varied in order to study the separate effects of rotational and translational degrees of freedom. A critical comparison of our results with the present analytical theories makes it possible to determine which aspects of the solvent structure and dynamics are still missing in the present forms of these theories.

II. THE SIMULATION

The simulated system is a Stockmayer liquid: 400 structureless particles characterized by point dipoles $\boldsymbol{\mu}$ and Lennard-Jones interactions, moving in a box (size L) with periodic boundary conditions. In addition, a solute atom A which can become an ion of charge q is imbedded in this solvent. The electrostatic potentials are handled within the effective dielectric environment scheme,[33] whereupon the interaction between particles α and β with $R_{\alpha\beta}<R_C$ is supplemented by an image potential arising from a continuum dielectric of dielectric constant ϵ' surrounding particle α at distance $\geqslant R_C$. In our simulations we take $R_C=L/2$. ϵ' is chosen to be self-consistent with the simulated system. The Lagrangian of the system is given by

$$\begin{aligned}L(\mathbf{R},\dot{R},\boldsymbol{\mu},\dot{\boldsymbol{\mu}}) &= \frac{1}{2}M_A\dot{R}_A^2+\frac{1}{2}M\sum_{i=1}^{N}\dot{R}_i^2+\frac{1}{2}\sum_{i=1}^{N}\frac{I}{\mu^2}\dot{\boldsymbol{\mu}}_i^2 \\ &\quad -\frac{1}{2}\sum_{i\neq j}^{N}V_{ij}^{\mathrm{LJ}}(R_{ij})-\sum_{i=1}^{N}V_{iA}^{\mathrm{LJ}}(R_{iA}) \\ &\quad -\frac{1}{2}\sum_{i\neq j}^{N}V^{\mathrm{DD}}(\mathbf{R}_i,\mathbf{R}_j,\boldsymbol{\mu}_i,\boldsymbol{\mu}_j) \\ &\quad -\sum_{i=1}^{N}V^{\mathrm{AD}}(\mathbf{R}_A,\mathbf{R}_i,\boldsymbol{\mu}_i)-\sum_{i=1}^{N}\lambda_i(\boldsymbol{\mu}_i^2-\mu^2), \qquad (4)\end{aligned}$$

where N is the number of solvent molecules of mass M, dipole moment μ, and moment of inertia I. $\mathbf{R}_A$ and $\mathbf{R}_i$ are positions of the impurity atom (that becomes an ion with charge q) and a solvent molecule, respectively, and R_{ij} is $|\mathbf{R}_i-\mathbf{R}_j|$. V^{LJ}, V^{DD}, and V^{AD} are, respectively, Lennard-Jones, dipole–dipole, and charge–dipole potentials, given by

$$V_{ij}^{\mathrm{LJ}}(R)=4\epsilon_D\left[(\sigma_D/R)^{12}-(\sigma_D/R)^6\right] \qquad (5)$$

(V_{iA}^{LJ} is of the same form with σ_A and ϵ_A replacing σ_D and ϵ_D) and

$$V^{\mathrm{DD}}(\mathbf{R}_i,\mathbf{R}_j,\boldsymbol{\mu}_i,\boldsymbol{\mu}_j)=\frac{\boldsymbol{\mu}_i\cdot\boldsymbol{\mu}_j-3(\mathbf{n}\cdot\boldsymbol{\mu}_i)(\mathbf{n}\cdot\boldsymbol{\mu}_j)}{R_{ij}^3}-\frac{2(\epsilon'-1)}{(2\epsilon'+1)R_C^3}\boldsymbol{\mu}_i\cdot\boldsymbol{\mu}_j, \qquad (6)$$

where $\mathbf{n}=(\mathbf{R}_i-\mathbf{R}_j)/R_{ij}$,

$$V^{\mathrm{AD}}(\mathbf{R}_i,\boldsymbol{\mu}_i,\mathbf{R}_A)=q\left(\frac{1}{R_{ij}^3}-\frac{2(\epsilon'-1)}{(2\epsilon'+1)R_C^3}\right)\boldsymbol{\mu}_i(\mathbf{R}_i-\mathbf{R}_A). \qquad (7)$$

The electrostatic potentials V^{DD} and V^{AD} also include reaction field terms.[33,34] The last term in Eq. (4) is included in the Lagrangian as a constraint, in order to preserve the magnitude of the dipole moments ($|\boldsymbol{\mu}_i|=\mu$) with a SHAKE like algorithm.[35] In this representation the mass M and the moment of inertia I of the solvent molecules are independent parameters, which makes it possible to study the relative importance of translational and rotational motions in the solvation process without affecting other potentially relevant parameters such as the molecular size. The time evolution is done using the velocity Verlet algorithm, with the value of $\lambda(t)$ determined as in the SHAKE algorithm, and with the Andersen[36] thermalization used to keep the system at constant temperature.

For the Stockmayer solvent, the molecular parameters were taken to approximate the CH_3Cl molecule: $\sigma_D=4.2$ Å, $\epsilon_D=195$ K, $M=50$ amu, $I=33.54$ amu Å^2, and $\mu=1.87$ D. The parameters taken for the ion in the simulations described later were $M_A=25$ amu, $\sigma_A=3.675$ Å, and $\epsilon_A=120$ K. q is taken to be one electron charge e. The simulation was done at 240 K. The edge length of the cubic simulation cell was $L=33.2$ Å, corresponding to the density $\rho=1.09\times10^{-2}$ Å^{-3} [the density of CH_3Cl at this temperature]. In reduced units we have $\rho^*\equiv\rho\sigma_D^3=0.81$, $\mu^*\equiv\mu/(\epsilon_D\sigma_d^3)^{1/2}=1.32$, $T^*\equiv k_BT/\epsilon_D=1.23$, and $I^*\equiv I/(M\sigma^2)=0.038$. A simple switching function

$$f(R)=\begin{cases}1 & R<R_S\\ (R-R)/(R_C-R_S) & R_S<R<R_C\\ 0 & R>R_C\end{cases} \qquad (8)$$

was used to smoothly cut off the electrostatic potential. In the present simulation we took $R_c=L/2$ and $R_s=0.95R_c$. Under these simulation conditions the pressure fluctuates in the range 500 ± 100 At. The dielectric constant ϵ is computed from pure solvent simulations, using the expression[33]

$$\frac{(\epsilon-1)(2\epsilon'+1)}{2\epsilon'+\epsilon}=\frac{1}{k_BTR_C^3}\langle\mathbf{P}\cdot\mathbf{P}(R_C)\rangle, \qquad (9)$$

where

$$\mathbf{P}=\sum_{i=1}^{N}\boldsymbol{\mu}_i \qquad (10a)$$

and

$$\mathbf{P}(R_C) = \frac{1}{N}\sum_{j=1}^{N}\sum_{k=1}^{N}{}' \boldsymbol{\mu}_k, \tag{10b}$$

where the prime on the inner summation indicates the restriction $R_{jk} < R_C$. The result for our solvent is ~ 17 [$\epsilon(CH_3Cl) = 12.6$ at 253 K]. After evaluating ϵ in this way and confirming that this is a self-consistent choice, we proceeded with $\epsilon' = \epsilon$. However, as discussed later our dynamical results are not sensitive to the magnitude of ϵ'.

The time evolution was carried out using a time step of 3 fs, which gave energy conservation to within 10^{-4} over $\sim 80\,000$ time steps. After equilibrating the system at 240 K, we have computed both the equilibrium correlation function $C(t)$ from equilibrium trajectories with both a charged ($q = e$) and an uncharged ($q = 0$) impurity atom, and the nonequilibrium solvation function $S(t)$ following a step function change from $q = 0$ to $q = e$. In addition to the CH_3Cl solvent model characterized by the parameters given, we have also carried out calculations for different values of the parameter[15]

$$p' = I/2M\sigma^2 \tag{11}$$

which measures the relative importance of rotational and translational solvent motions.

With the model described earlier we have conducted a series of solvation dynamics studies. Our results are described in Sec. III.

III. RESULTS

Figure 1 shows the equilibrium solvent induced electrostatic potential V at the position of the ion, as a function of the ion charge q. Clearly the solvent response is linear with q all the way up to $q = e$, the charge considered in this study. The slope of the straight line in Fig. 1 is 4.4. The corresponding slope from the Born solvation theory, if we take the ion radius to be $\sigma_A/2$, is 7.4. The MSA theory predicts (using σ_A and σ_D for the diameters of the ion and the solvent, respectively) a slope of 4.6.

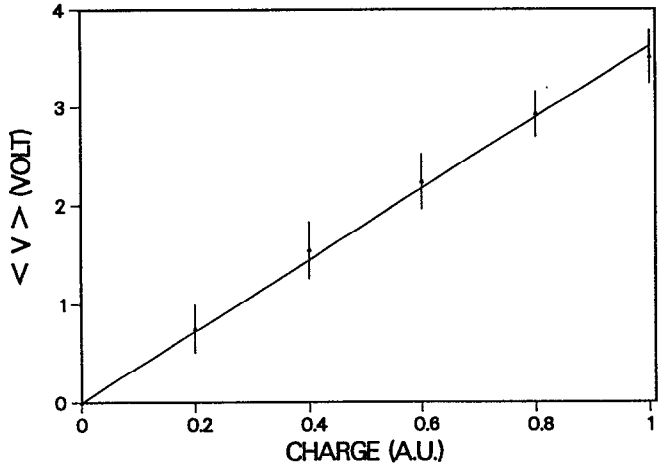

FIG. 1. The electrostatic response potential $\langle V \rangle$ induced by the solvent at the position of the solute ion, as a function of the solute charge.

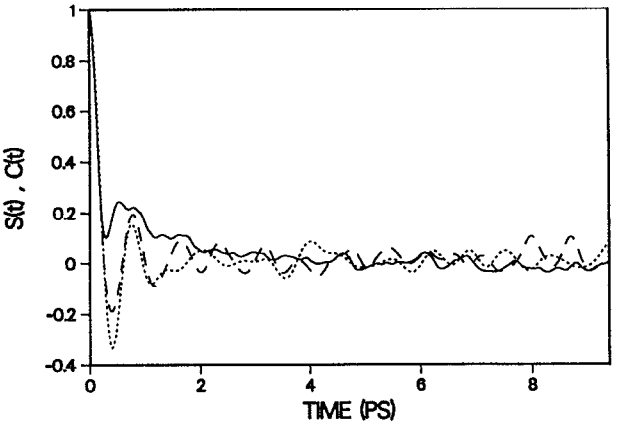

FIG. 2. The equilibrium relaxation functions $C(t)$ [Eq. (2); dashed and dotted lines] and $S(t)$ [Eq. (3); solid line] obtained as described in the text. In the nonequilibrium simulation the ion charge is switched on at $t = 0$. The dotted and dashed lines represent $C(t)$ obtained from equilibrium simulations with uncharged and charged ion, respectively.

Figure 2 shows the time evolution of the solvation functions $C(t)$ [Eq. (2)] and $S(t)$ [Eq. (3)]. The equilibrium results are evaluated from an equilibrium trajectory of 220 ps for a system consisting of the solvent and a charged or uncharged atom. The nonequilibrium results are averages over 25 different trajectories, each starting from an initial configuration taken from an equilibrium run of an all-neutral system (at 65 ps intervals[37]) following switching of the charge on the impurity atom from $q = 0$ to $q = e$.

As observed before in other systems,[2,27] there is a large degree of similarity between the equilibrium and nonequilibrium results. Both consist of an initial, apparently inertial, part followed by a relatively slow residual relaxation. However, the initial inertial part is more pronounced in $C(t)$. The latter is also characterized by stronger oscillations in the residual part of the relaxation. The inertial origin of these oscillations was recently discussed by Maroncelli.[2]

In Fig. 3 we check the sensitivity of our results to the

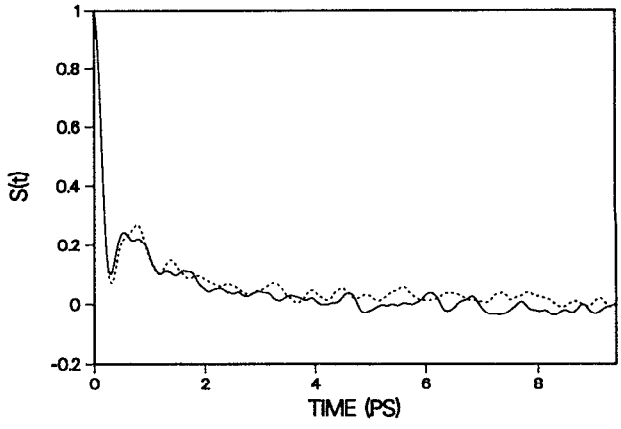

FIG. 3. The function $S(t)$ obtained with $\epsilon' = 17.0$ (solid line, same as in Fig. 2), together with the same function obtained with $\epsilon' = 1.0$ (dashed line). ϵ' is the continuum dielectric constant associated with our reaction field boundary conditions.

present choice of boundary conditions. We note that the use of reaction field boundary conditions as implemented here is strictly valid only for equilibrium simulations, since the *dynamic* response of the dielectric continuum at $R > R_c$ is not taken into account. One could argue that for the short-time phenomena considered here, ϵ' should have been taken smaller then the static dielectric constant of the system. Figure 3 shows that on the relevant time scale our dynamical results do not change if we take $\epsilon' = 1$ instead of $\epsilon' = \epsilon = 17$. (The absolute solvation energy does depend on ϵ', and replacing $\epsilon' = 17$ by $\epsilon' = 1$ changes it by $\cong 5\%$.)

In the simulations described so far the solvent parameters are given by the aforementioned data. For these, the dimensionless parameter p', Eq. (11) is 0.019. In order to separate between the effects of the solvent translational and rotational degrees of freedom, we have also studied systems characterized by the p values 0, 0.125, 0.25, and ∞. Except for $p' = 0$, these values were obtained by changing I, keeping $M = 50$ amu. The value $p' = 0$ was achieved by taking $M = M_A = \infty$ and $I = 33.54$ amu Å^2. Note that the values $p' = 0$ and $p' = \infty$ correspond to models with frozen translations and frozen rotations, respectively.

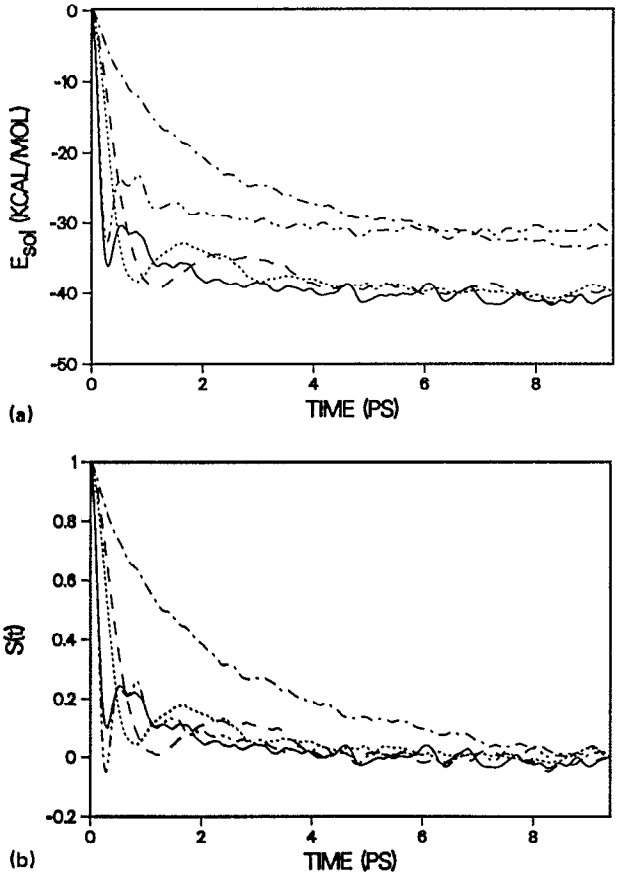

FIG. 4. The solvation energy E_{sol} [Fig. 4(a)] and the nonequilibrium solvation function S [Fig. 4(b)], plotted against time (after switching the ion charge from 0 to e) for different solvent models characterized by the parameter p' [Eq. (11)]. Solid double-dotted line, $p' = 0$; solid line, $p' = 0.019$; dotted line, $p' = 0.125$; dashed line, $p' = 0.25$; solid dotted line, $p' = \infty$.

TABLE I. Relaxation times τ obtained from fitting the solvation energy at short time to the function $E(t) = A\{\exp[-(t/\tau)^2] - 1\}$. The fitting is done in the range $S(t) > 0.3$.

p'	M (amu)	I (amu Å^2)	τ (ps)	Å
0.0	∞	33.54	0.206	48
0.019	50	33.54	0.170	41
0.125	50	220.5	0.347	36
0.250	50	441.0	0.421	32

Figures 4(a) and 4(b) show, respectively, the solvation energy $E_{sol}(t)$ and the nonequilibrium solvation function $S(t)$ obtained for these different systems. The following points are observed.

The asymptotic ($t \to \infty$) values of E_{sol} [Fig. 4(a)] are different in the cases $p' = 0$ ($M = \infty$) and $p' = \infty$ ($I = \infty$) then in the other cases because of the freezing of solvent translations and rotations, respectively. Note, however, that the $I = \infty$ curves converge very slowly (the solvent compensates for the lack of rotations by bringing into the neighborhood of the solute solvent molecules with the "correct" orientation) and probably did not reach its asymptotic value in Fig. 4(a).

Except for the rotationless system ($p' = \infty$), all the other systems exhibit a bimodal relaxation, with a fast relaxation component which accounts for most of the solvation energy.

The relaxation of the rotationless solvent is exponential [a fit to $\exp(-t/\tau)$ yields $\tau = 2.2$ ps].

A closer look at the fast component in the finite p' systems shows a Gaussian behavior, a fit to $\exp[-(t/\tau)^2]$ yields the τ values summarized in Table I. τ increases with increasing solvent moment of inertia (recall that this is how p' is changed for $p' > 0$), still for the range of p' studied, it stays distinct from the long component. Note that the system with $p' = 0$ cannot be directly compared in this respect with the other systems because, in this case, the solvent mass was taken to be infinite.

The inertial oscillations and the thermal noise seen in the relatively small slow relaxation component make it difficult to estimate the long relaxation time. A fit for the $p' = 0.019$ case yields $\tau \cong 2.7 \pm 0.7$ ps. The long-time components in the other systems relax on similar time scales.

The relative contributions of different solvation shells to the solvation process were obtained by considering solvent layers defined according to the minima observed in the solvent–solute radial distribution function. Distinct minima in the solvent density are observed at distances of 5.5 and 10.0 Å (± 0.3 Å) from the ion center, and these were used to define the solvation shells. Averaging the number of solvent particles within these distances, we have defined the first solvation shell as that containing the eight solvent molecules nearest to the ion and the second solvation shell as that containing the next-nearest 26 molecules. The remaining solvent molecules constitute the third shell.

Our results on the separate contributions of these shells to the solvation process are depicted in Figs. 5–7. The solva-

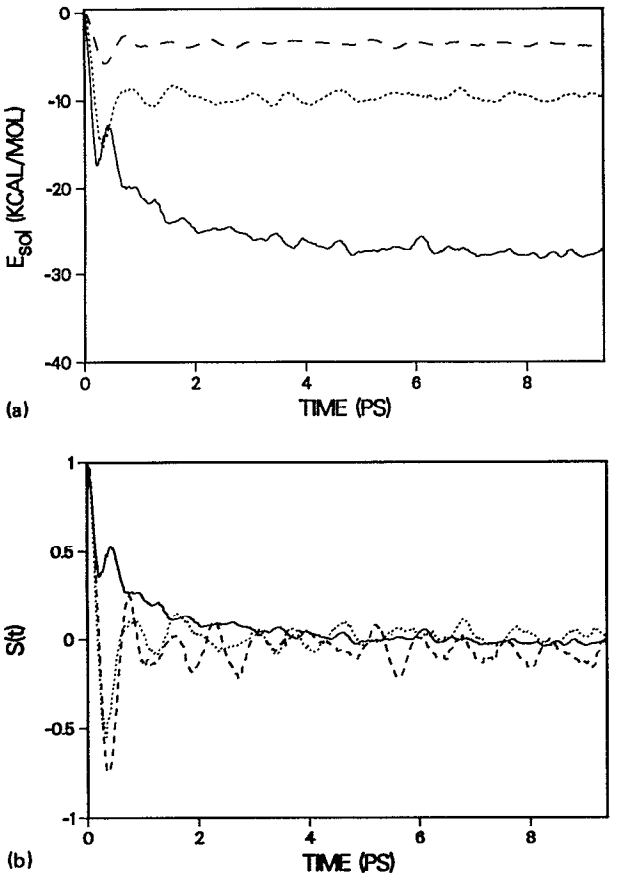

FIG. 5. (a) The solvation energy and (b) the function $S(t)$ associated with the three solvation shells defined in the text, plotted against time after the ion charge is switched on, for the system with $p' = 0.019$. Solid line, nearest shell; dotted line, second shell; dashed line, outer shell.

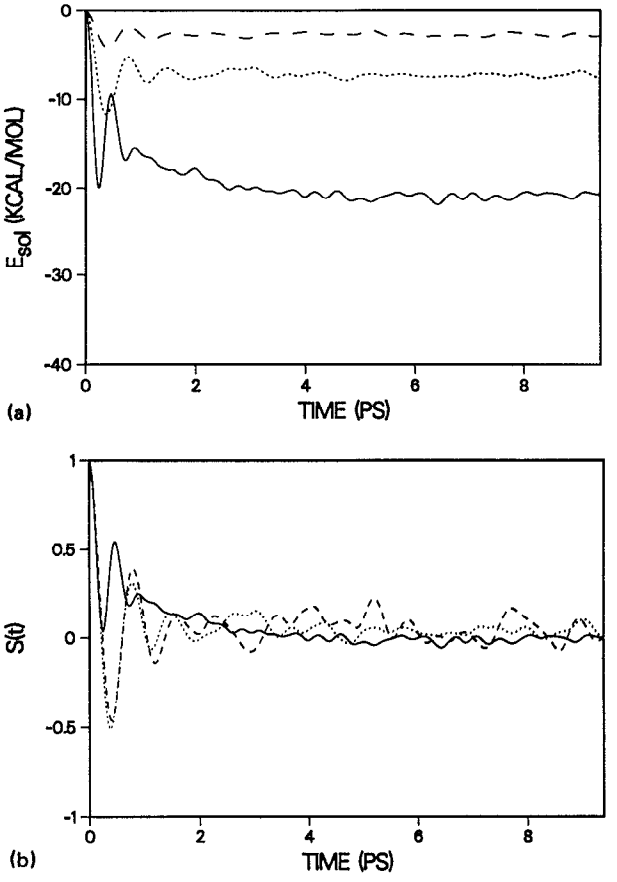

FIG. 6. Same as Fig. 5, for the translationless case ($p' = 0$).

tion shells were defined using the pair correlation function at $t = \infty$; however, the assignment of atoms to the different shells were determined by their instantaneous positions. Figures 5(a) and 5(b) show the time evolution of the solvation energies and of the functions $S(t)$ associated with the different shells, for the original CH_3Cl parameters ($p' = 0.019$). Figures 6 and 7 show similar results for the systems with frozen translations ($p' = 0.0$) and inhibited rotations ($p' = 0.25$). The behavior in all these cases is qualitatively similar. (a) The solvation energy is dominated by the first solvation shell. When both translations and rotations are active (Figs. 5 and 7) the first, second, and third shells contribute $\sim 67\%$, 24%, and 9%, respectively, to the solvation energy. The fast, inertial relaxation component is seen in all three shells and altogether accounts for $\sim 80\%$ of the solvation energy. Inertial oscillations are seen in the long-time component of the time evolution. These oscillations, most pronounced in the $S(t)$ functions, correspond to low amplitude librations about the final average orientations of the solvent molecules (see, e.g., Fig. 8). Interestingly, it appears that relaxation of inertial effects is faster near the ion, and is slowest (6–8 ps) for the molecules in the outer layers. This issue deserves further study. The nearest solvation shell exhibits a pronounced slow relaxation component, which is weaker or absent in the outer shells.

Finally, the nature of the motion that gives rise to the fast relaxation component is seen in Fig. 8, where we plot as functions of time the average angles between the molecular dipoles in the different solvation shells and between the corresponding radius vectors to the ion centers. These results are for the $p' = 0.019$ system; the other systems with $p' < \infty$ show qualitatively similar behavior. Generally, the angular time evolution is similar to that of the solvation energy. Typical to the present structureless system and in contrast to the observation in more structured solvents, the fast relaxation component is associated with a large amplitude of the angular motion.

IV. DISCUSSION AND CONCLUSION

The present study was motivated by our desire to examine a system that, while maintaining a relatively realistic character, is closer in nature to the theoretical models used in recent years to study solvation dynamics. Our results indicate that even in this simple system most of these theories still do not provide an adequate description. The inertial component, initially thought to characterize H-bonded solvents,[22,23] and later associated with librational motion in structured solvents,[2] is seen to be very important also in the present case of structureless solvent. As seen in Fig. 8, this component arises in the present system from a large amplitude rotational motion. The average angle of molecules in

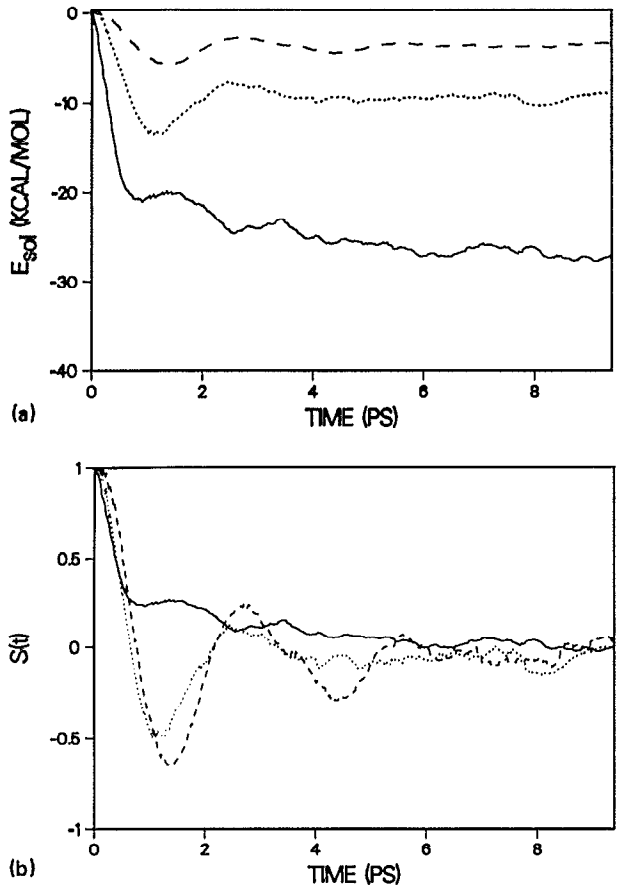

FIG. 7. Same as Fig. 5, for $p' = 0.25$.

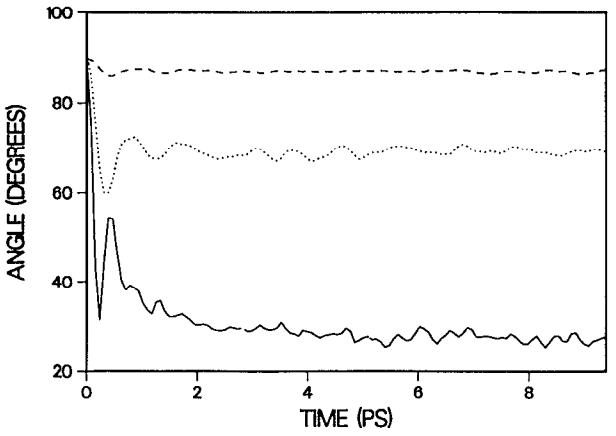

FIG. 8. The time dependence of the average angle between the molecular dipoles and between the corresponding radius vectors to the ion center, associated with molecules in the three different solvation shells defined in the text, plotted against time following the switching on of the ionic charge.

the first solvation shell (for the $p = 0.019$ system) evolves from 90° to ~30° in about 0.15 ps. This should be contrasted with the simulation results in the more structured water and acetonitrile systems, where the fast relaxation component appears to be associated with small amplitude librations of the nearest-neighbor solvent molecules. The overall effect on the solvation process is however very similar.

A close look at the short-time evolutions of the three solvation layers in Figs. 5(a) and 8 reveals more details of this initial energy flow. It is seen that the response of the second shell is somewhat delayed relative to that of the first one and, similarly, the third shell follows somewhat after the second. The relaxation on this time scale clearly proceeds from the inside outwards. It is important to note that this behavior is seen also for the purely rotational ($M = \infty$, $p' = 0$) system [Fig. 6(a)].

The only feature in the present simulation results which is reminiscent of the predictions of the Onsager, MSA, or the GDE theories of solvation is the appearance of a long-time relaxation component associated with the first solvation shell. It is tempting to associate this component, which is weak or unresolved in the relaxation of the outer layers, with the recently popularized Onsager "inverse snowball" picture. We note, however, that it accounts for only a small part (~20%) of the of the total solvation energy, and its presence is equally pronounced in the translationless ($p' = 0$) system as in a system with a considerable translational motion ($p' = 0.25$). This suggests that the slow component in the relaxation of the first solvation shell is associated with residual diffusive energy flow out of this shell, as suggested by Maroncelli.[2]

Recent theoretical treatments of solvation dynamics, outlined in Sec. I, predict nonexponential relaxation of the solvation energy, with relaxation times ranging between the transversal and longitudinal dielectric relaxation time of the solvent. A rough estimate of the longitudinal relaxation time in our $p' = 0.019$ system yields a value ~1.5–2 shorter than the short-time Gaussian relaxation time ($\tau = 0.17$ ps, cf. Table I) of this system. τ_L is a many-body macroscopic property of the dielectric solvent, and the features associated with the fast relaxation time as described earlier clearly indicate that there is no direct relationship between these quantities.

In conclusion, solvation dynamics in the structureless Stockmayer liquid is qualitatively very similar to that observed in earlier studies of more structured polar solvents. This remains true even in the limit where translations are frozen, which was expected to be the closest in character to the original models used by the MSA and the GDE theories of solvation. The importance of inertial motions on the subpicosecond time scale thus seems to be a general feature of the solvation process in small molecule solvents. While inertial motions are expected to affect the short-time response of such solvents, it is both surprising and significant that these motions dominate the solvation dynamics (and, therefore, related chemical processes in solution) in all solvent models studied so far. Since linear response provides a good approximation for a large range of parameters (at least for $q = e$), it is expected that generalized dielectric theories should be able to approximately describe these phenomena, provided that inertial response is incorporated into the large k and ω part of the solvent dielectric function.

While this paper was being prepared for publication we learned of similar work by Berkowitz and co-workers.[38] They have also studied solvation dynamics in a Stockmayer fluid with a different choice of interaction parameters. Their observations are qualitatively similar to ours.

ACKNOWLEDGMENTS

This work was supported by the Commission for Basic Research of the Israel Academy of Science, and by the U.S.A–Israel Binational Science Foundation. The work was initiated when both authors were visiting the School of Physics at Georgia Institute of Technology. We thank Professor U. Landman and Dr. R. N. Barnett for many useful discussion and for technical help. A. N. also thanks Professor J. Ford for his assistance.

[1] B. Bagchi, Ann. Rev. Phys. Chem. **40**, 115 (1989), and references therein.
[2] M. Maroncelli, J. Chem. Phys. **94**, 2084 (1991), and references therein.
[3] W. Jarzeba, G. C. Walker, A. E. Johnson, and P. F. Barbara, Chem. Phys. **152**, 57 (1991), and references therein.
[4] G. Van Der Zwan and J. T. Hynes, J. Chem. Phys. **78**, 4174 (1983).
[5] G. Van Der Zwan and J. T. Hynes, J. Phys. Chem. **89**, 4181 (1985).
[6] P. G. Wolynes, J. Chem. Phys. **86**, 5133 (1987).
[7] I. Rips, J. Klafter, and J. Jortner, J. Chem. Phys. **88**, 3246 (1988).
[8] I. Rips, J. Klafter, and J. Jortner, J. Chem. Phys. **89**, 4288 (1988).
[9] A. L. Nichols III and D. F. Calef, J. Chem. Phys. **89**, 3783 (1988).
[10] D. F. Calef and P. G. Wolynes, J. Chem. Phys. **78**, 4145 (1983).
[11] B. Bagchi and A. Chandra, J. Chem. Phys. **90**, 7338 (1989).
[12] A. Chandra and B. Bagchi, J. Chem. Phys. **91**, 2594 (1989).
[13] B Bagchi and A. Chandra, Chem. Phys. Lett. **151**, 47 (1988).
[14] R. F. Loring and S. Mukamel, J. Chem. Phys. **87**, 1272 (1987).
[15] L. E. Fried and S. Mukamel, J. Chem. Phys. **93**, 932 (1990).
[16] A. A. Kornyshev, A. M. Kuznetsov, D. K. Phelps, and M. J. Weaver, J. Chem. Phys. **91**, 7159 (1989).
[17] E. W. Castner, Jr., G. R. Fleming, B. Bagchi, and M. Maroncelli, J. Chem. Phys. **89**, 3519 (1988).
[18] D. Wei and G. N. Patey, J. Chem. Phys. **91**, 7113 (1989); **93**, 7113 (1990).
[19] F. O. Raineri, Y. Zhou, H. L. Friedman, and G. Stell, Chem. Phys. **152**, 201 (1991).
[20] A. Chandra and B. Bagchi, J. Chem. Phys. **94**, 3177 (1991); Chem. Phys. **156**, 323 (1991); Proc. Ind. Acad. Sci. **103**, 77 (1991).
[21] S. Engström, B. Jönsson, and R. W. Impey, J. Chem. Phys. **80**, 5481 (1984).
[22] M. Maroncelli and G. R. Fleming, J. Chem. Phys. **89**, 5044 (1988).
[23] R. N. Barnett, U. Landman, and A. Nitzan, J. Chem. Phys. **90**, 4413 (1990).
[24] P. J. Rossky and J. Schnitker, J. Phys. Chem. **92**, 4277 (1988).
[25] O. A. Karim, A. D. J. Haymet, M. J. Banet, and J. D. Simon, J. Phys. Chem. **92**, 3391 (1988).
[26] J. S. Bader and D. Chandler, Chem. Phys. Lett. **157**, 501 (1989).
[27] E. A. Carter and J. T. Hynes, J. Chem. Phys. **94**, 5961 (1991).
[28] T. Fonseca and B. M. Ladanyi, J. Phys. Chem. **95**, 2116 (1991).
[29] L. Onsager, Can J. Chem. **55**, 1819 (1977).
[30] E. W. Castner, M. Maroncelli, and G. R. Fleming, J. Chem. Phys. **86**, 1090 (1987); M. Maroncelli and G. R. Fleming, *ibid.* **86**, 6221 (1987).
[31] S. J. Rosenthal, X. Xie, M. Du, and G. R. Fleming, J. Chem. Phys. **94**, 4715 (1991).
[32] For recent simulations on dielectric properties of Stockmayer fluids, see E. L. Pollock and B. J. Alder, Physica **102A**, 1 (1980); Phys. Rev. Lett. **46**, 950 (1981); M. Neumann and O. Steinhauser, Chem. Phys. Lett. **102**, 508 (1983); M. Neumann, O. Steinhauser, and G. S. Pawley, Mol. Phys. **52**, 97 (1984).
[33] J. W. de Leeuw, J. W. Perram, and E. R. Smith, Annu. Rev. Phys. Chem. **37**, 245 (1986).
[34] C. J. F. Böttcher and P. Bordewijc, *Theory of Electric Polarization*, 2nd ed. (Elsevier, Amsterdam, 1978), Vol. 2, Chap. 10.
[35] M. P. Allen and D. J. Tildesely, *Computer Simulation of Liquids* (Oxford, London, 1989).
[36] H. C. Andersen, J. Chem. Phys. **72**, 2384 (1980).
[37] Within these large time intervals, the first 50 ps where done with a time step of 15 fs, 5 times longer then our standard timestep.
[38] L Perera and M. Berkowitz, J. Chem. Phys. (to be published).